Interplay between Phonons and Anisotropic Elasticity Drives Negative Thermal Expansion in PbTiO_{3}

Ethan T. Ritz and Nicole A. Benedek

Interplay Between Phonons and Anisotropic Elasticity Drives Negative Thermal Expansion in PbTiO

Ethan T. Ritz[1, *] and Nicole A. Benedek[2, †]

Sibley School of Mechanical and Aerospace Engineering, Cornell University, Ithaca, NY 14853 US
[2]*Department of Materials Science and Engineering, Cornell University, Ithaca, NY 14853 US*

(Dated: October 8, 2018)

We use first-principles theory to show that the ingredients assumed to be essential to the occurrence of negative thermal expansion (NTE) – rigid unit phonon modes with negative Grüneisen parameters – are neither sufficient nor necessary for a material to undergo NTE. Instead, we find that NTE in $PbTiO_3$ involves a delicate interplay between the phonon properties of a material (Grüneisen parameters) and its anisotropic elasticity. These unique insights open new avenues in our fundamental understanding of the thermal properties of materials, and in the search for NTE in new materials classes.

The first report of negative thermal expansion (NTE) in solids appeared in 1907, with Scheel's observations that quartz and vitreous silica shrink upon heating [1, 2]. NTE has since been observed in essentially every materials class, including metals [3], polymers [4], metal-organic frameworks [5–7], and semiconductors [8–10]. However, despite over a century of study [11–13], the microscopic mechanisms of NTE remain poorly understood in all but a handful of cases [14, 15].

In inorganic framework materials, so-called rigid unit phonon modes (RUMs) [16, 17] are widely recognized as being important drivers of NTE. Rather than longitudinal stretching of bonds, these modes typically shorten metal-metal bond distances as temperature increases through relative rotations of rigid (or almost rigid) polyhedral groups, or kinking of oxygen-metal-oxygen bond networks. The RUM model of NTE successfully accounts for the thermal behavior of the canonical NTE material ZrW_2O_8 [14, 18, 19], as well as a number of zeolites [20, 21] and Prussian blue materials [22]. A second essential ingredient for the occurrence of NTE appears to be the existence of low-frequency RUMs with large, negative Grüneisen parameters, that is, modes with frequencies that *decrease* with decreasing volume. In fact, negative Grüneisen parameters are sometimes claimed to be prerequisites for NTE behavior [23, 24]. Indeed, as far as we know, the only exceptions are the elemental metals Zn [25], Cd [25], As [26], and Sb [26], all of which exhibit only uniaxial, rather than volumetric, NTE.

Given the apparent importance of RUMs and phonons with negative Grüneisen parameters, it is curiously rare for ABO_3 perovskites to undergo NTE. Most perovskites undergo one or more structural phase transitions involving phonons with strong RUM-like character (typically rotations of the BO_6 octahedra), and these types of modes are associated with negative Grüneisen parameters in, for example, β-cristobalite, β-quartz, and ZrW_2O_8 [27]. In contrast, recent work [28, 29] has shown that (uniaxial) NTE is common in *layered* perovskites, such as Ruddlesden-Popper phases, because the combined effects of layering and rotations of the BO_6 octahedra enhance their elastic anisotropy compared to bulk perovskites; this enhanced elastic anisotropy appears to be the origin of uniaxial NTE in layered perovskites. Of course, bulk perovskites may exhibit elastic anisotropy, as Refs. 28 and 29 acknowledge, however the magnitude of the anisotropy is generally not large enough to induce NTE.

In this Letter, we use the ferroelectric perovskite $PbTiO_3$ to demonstrate that neither RUMs nor phonons with negative Grüneisen parameters are necessary (or sufficient) in order for a material to undergo NTE. A key discovery we make is that in non-cubic materials, NTE cannot be predicted based on either the signs or magnitudes of an individual Grüneisen parameter or elastic constant by itself, as is commonly assumed. In these systems, the thermal expansion along a given axis is coupled to multiple Grüneisen parameters through multiple *independent* elastic constants. We use theory and first-principles calculations to elucidate the microscopic mechanism of NTE in $PbTiO_3$ and show that few of the modes critical to driving NTE have negative Grüneisen parameters and that they are not RUMs, even though $PbTiO_3$ contains many RUM-like modes [20]. We then connect the physical mechanism of NTE in $PbTiO_3$ to its electronic structure, and show that its elastic properties are dominated by the stereochemical activity of the Pb^{2+} $6s^2 6p^0$ lone electron pair. Our results are striking because they suggest that $PbTiO_3$ is unique among well-studied NTE materials, and appears to be the only material that exhibits *volumetric* NTE well above room temperature, and with positive Grüneisen parameters along all unique crystallographic axes. These results bring clarity to the driving mechanism of NTE in $PbTiO_3$, and broaden the search for new NTE systems to include materials overlooked in the past due to a lack of large, negative Grüneisen parameters.

$PbTiO_3$ is cubic at high temperatures but undergoes a phase transition at 760 K to a tetragonal ($P4mm$) ferroelectric phase; this phase exhibits volumetric NTE down to approximately room temperature (though only the c axis decreases with temperature while the a axes increase,
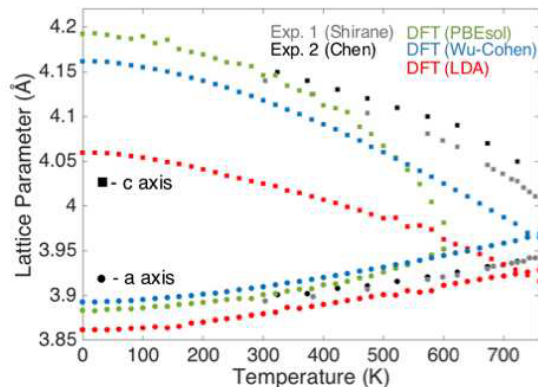
FIG. 1. (Color online) Lattice parameters (a filled circles, c filled squares) as a function of temperature from first-principles calculations (colored icons) and from experiment (black and gray icons [35, 36]).

the net effect is a decrease in volume). We used density functional theory, as implemented in Quantum Espresso with GBRV pseudopotentials [30, 31] (see Supplementary Information (SI) for methods and convergence critera) to calculate the evolution of lattice parameters as a function of temperature in the quasiharmonic approximation (QHA). Figure 1 compares our results obtained from three functionals: LDA [32], PBEsol [33] and Wu-Cohen (WC) [34]. As expected, all three functionals slightly underestimate the lattice parameters, however each qualitatively reproduces the experimental trend of a lengthening c axis and shrinking a axis as temperature increases. Our calculations reproduce the experimentally observed volumetric NTE, and additional comparisons between data from our first-principles calculations and available experimental data for finite-temperature phonon dynamics and elastic constants indicate that the QHA is a justified approximation for this system (see SI). We report all remaining results for the WC functional only, since it best captures the structural properties of $PbTiO_3$. With this functional, we calculate a volumetric expansion coefficient α_v of -2.29×10^{-5} K^{-1} between 500 K and 700 K, which compares favorably with $\alpha_v = -1.8 \times 10^{-5}$ K^{-1} and -1.99×10^{-5} K^{-1} from [35] and [36], respectively.

We now turn to elucidating the microscopic mechanism of NTE in $PbTiO_3$. We first calculated the Grüneisen parameters for the equilibrium structure of $PbTiO_3$ at 300 K. Since $PbTiO_3$ is not cubic, the Grüneisen parameter γ has a tensor form,

$$\gamma_{s,\mathbf{k}}^{ij} \equiv -\frac{1}{\omega_{s,\mathbf{k}}}\frac{\partial \omega_{s,\mathbf{k}}}{\partial \varepsilon_{ij}}, \tag{1}$$

where $\omega_{s,\mathbf{k}}$ is the frequency of mode s at wavevector $\mathbf{k}$, ε_{ij} is a strain consistent with crystal symmetry, and i and j are Cartesian directions. We calculated $\gamma_{s,\mathbf{k}}^{ij}$ using a central difference, which required three separate calculations of the full dispersion curve. The quantity usually

referred to as the 'bulk' Grüneisen parameter is then defined as [37],

$$\gamma_{b,\mathbf{lk}}^{ij} = \frac{\sum_{s,\mathbf{k}} \gamma_{s,\mathbf{k}}^{ij} c_{s,\mathbf{k}}}{\sum_{s,\mathbf{k}} c_{s,\mathbf{k}}}, \tag{2}$$

where $c_{s,\mathbf{k}}$ is the mode specific heat at constant configuration. We note that the uniaxial stress perturbation method [38] could be suited to high-throughput studies to screen for NTE along particular axes, and to provide a quick alternative method to compare with results obtained using the strain perturbative definitions as in Eq. (1).

Figure 2 shows phonon dispersion curves for $PbTiO_3$ at 300 K with the magnitude and sign of $\gamma_{s,\mathbf{k}}^{a} \equiv \gamma_{s,\mathbf{k}}^{11}$ and $\gamma_{s,\mathbf{k}}^{c} \equiv \gamma_{s,\mathbf{k}}^{33}$ represented by the thickness and color of the band, respectively. Despite the presence of NTE, both bulk Grüneisen parameters are positive, $\gamma_{b,\mathbf{lk}}^{a} = 1.42$ and $\gamma_{b,\mathbf{lk}}^{c} = 0.40$. The density of states in Figure 2 indicates that the individual phonon modes contributing most strongly to $\gamma_{b,\mathbf{lk}}^{a}$ and $\gamma_{b,\mathbf{lk}}^{c}$ are low frequency modes with *positive* Grüneisen parameters, in contrast with the usual expectation that modes with large, negative mode Grüneisen parameters drive NTE. As shown in the Supplementary Information, if we force all modes below 100 cm^{-1} to be perfectly harmonic by keeping their frequencies constant with temperature, while allowing the frequencies of all other modes to change, then NTE behavior is completely suppressed. Hence, these low-frequency modes appear to be the primary drivers of NTE and of the positive bulk Grüneisen parameters along both the a and c axes. Additionally, Figure 3 shows that none of the distortions associated with the critical low-frequency modes are RUMs; they are instead dominated by translational Pb motion. [39] Our work so far raises two questions: how do we account for NTE in $PbTiO_3$, given the positive Grüneisen parameters, and do electronic effects play a role in NTE in this material?

Although large, negative mode Grüneisen parameters have been associated with NTE in the literature, this relationship need not hold for anisotropic systems. In cubic materials, the bulk Grüneisen parameter is scalar and the coefficient of volumetric thermal expansion can be expressed as [40]

$$\alpha_v = \frac{\gamma_{b,\mathbf{lk}} C_\eta}{3B}, \tag{3}$$

where B is the bulk modulus and C_η is the specific heat at constant configuration. The bulk Grüneisen parameter $\gamma_{b,\mathbf{lk}}$ is still defined as in Eq. (2), however the individual mode Grüneisen parameters are reduced to simple volume derivatives,

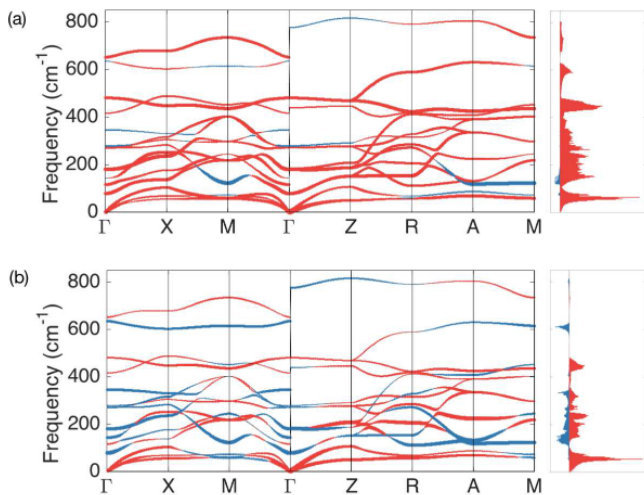$$\gamma_{s,\mathbf{k}} \equiv -\frac{V}{\omega_{s,\mathbf{k}}}\frac{d\omega_{s,\mathbf{k}}}{dV}. \tag{4}$$

FIG. 2. (Color online) **(a)** Phonon dispersion curve for PbTiO$_3$ at 300 K with band thickness proportional to the magnitude of γ^a for each mode, and color corresponding to sign of γ^a (red positive, blue negative). To the right is the sum of γ^a across entire Brillouin zone for each energy level at 300 K, positive (red) and negative (blue) contributions plotted separately. **(b)** Same, corresponding to γ^c.
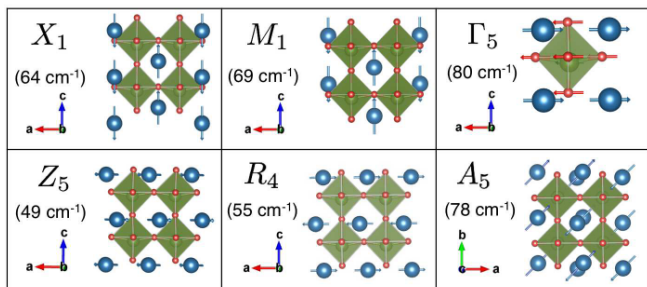

FIG. 3. (Color online) Representative set of distortions associated with low-frequency ($\omega < 100$ cm^{-1}) phonons for the indicated irreducible representation of each high symmetry point. Note the absence of RUMs and dominance of Pb motion. See SI for additional modes.

Looking at Eq. (3), $\gamma_{\text{b lk}}$ is the only term on the right-hand side that can be negative. Hence, a negative α_v in *cubic* systems is impossible without a negative $\gamma_{\text{b lk}}$, which must itself arise from large, negative mode Grüneisen parameters.

nisotropic materials have additional structural degrees of freedom that complicate the relationship between the coefficient of thermal expansion, Grüneisen parameters, and elastic constants. For example, in tetragonal systems like PbTiO$_3$, the coefficients of thermal expansion along a (α_a) and c (α_c) are defined as [41, 42]:

$$\alpha_a = (C_\eta/V)\left[(S_{11} + S_{12})\gamma^a_{\text{b lk}} + S_{13}\gamma^c_{\text{b lk}}\right], \quad (5)$$

and

$$\alpha_c = (C_\eta/V)\left[2S_{13}\gamma^a_{\text{b lk}} + S_{33}\gamma^c_{\text{b lk}}\right], \quad (6)$$

where S_{ij} is the ij^{th} component of the elastic compliance tensor in Voigt notation. Since $\alpha_v \equiv 2\alpha_a + \alpha_c$ [41], in order for α_v to be negative, we require

$$2(S_{11} + S_{12} + S_{13})\gamma^a_{\text{b lk}} + (S_{33} + 2S_{13})\gamma^c_{\text{b lk}} < 0. \quad (7)$$

Eq. (7) shows that negative bulk Grüneisen parameters are not a prerequisite for NTE in anisotropic materials. The S$_{ij}$ can be positive or negative, and the relative sign and magnitude of these terms constrain the signs of $\gamma^a_{\text{b lk}}$ and $\gamma^c_{\text{b lk}}$ required for NTE. Without knowledge of the full compliance tensor, o defi itive stateme ts about how the sig s or mag itudes of $\gamma^a_{\text{b lk}}$ a d $\gamma^c_{\text{b lk}}$ relate to α_v ca be made. However, the dependence of α_v on $\gamma^c_{\text{b lk}}$ and $\gamma^a_{\text{b lk}}$ can be determined directly if S$_{ij}$ is known.

Table I shows selected elements of the compliance tensor for the tetragonal phase of PbTiO$_3$ from first principles calculations, which compare well with experiment [43] (note the large magnitude of S_{13}, previously correlated [5, 28] with NTE behavior). The a-axis expands as temperature rises, and so α_a is positive. From Eq. (5), since $S_{11} + S_{12} > 0$ for PbTiO$_3$, $\gamma^a_{\text{b lk}}$ must be large and positive in order for $\alpha_a > 0$. Since positive Grüneisen parameters are known to be associated with positive thermal expansion, our results so far are unsurprising. However, we will now argue that it is the tendency of PbTiO$_3$ to expand along a with increasing temperature that *drives* the system to shrink along c, giving rise to volumetric NTE.

The key to understanding NTE in PbTiO$_3$ is to examine the relationship between the Grüneisen parameters, and applied stress along the a axis and induced strain along the c axis. Since the c axis contracts as temperature increases, $\alpha_c < 0$. The conventional wisdom suggests that this requires a negative $\gamma^c_{\text{b lk}}$, while we know that $\gamma^c_{\text{b lk}}$ is actually positive in this system. From Eq. (6), since S_{33} is also positive, the only way for α_c to be negative is for the product $S_{13}\gamma^a_{\text{b lk}}$ to be negative – indeed the case for PbTiO$_3$, as shown in Table I. Physically, a large, negative S_{13} in tetragonal systems functions in a similar way to a large, positive Poisson's ratio in cubic systems. *It is this temperature-i duced egative strai that drives α_c to be egative, a d gives rise to NTE i PbTiO$_3$.*

If $S_{13}\gamma^a_{\text{b lk}}$ was positive, or even slightly less negative, then it would be energetically favorable for the c axis to expand with increasing temperature. Hence, the NTE is not due to a c axis driven to contract by a negative $\gamma^c_{\text{b lk}}$, but i spite of a positive $\gamma^c_{\text{b lk}}$. We illustrate this by rewriting equations 5 and 6 in matrix form:

TABLE I. Selected elements of the compliance tensor for PbTiO₃ and SnTiO₃ from first-principles calculations in units of 10^{-3} GPa^{-1}.

	S_{11}	S_{12}	S_{13}	S_{33}
PbTiO₃	7.44	0.49	-11.94	55.69
SnTiO₃	7.79	-1.45	-6.83	31.36

$$\begin{bmatrix} \alpha_a \\ \alpha_a \\ \alpha_c \end{bmatrix} = \begin{bmatrix} S_{11} & S_{12} & S_{13} \\ S_{12} & S_{11} & S_{13} \\ S_{13} & S_{13} & S_{33} \end{bmatrix} \begin{bmatrix} \frac{\eta \gamma_{\text{blk}}^a}{V} \\ \frac{\eta \gamma_{\text{blk}}^a}{V} \\ \frac{\eta \gamma_{\text{blk}}^c}{V} \end{bmatrix}. \tag{8}$$

The column vector on the right has units of pressure/Kelvin – a temperature-induced stress – linked through the compliance tensor to the column vector on the left, which has units of strain/Kelvin. In this arrangement, γ_{blk}^a and γ_{blk}^c define the magnitude of a thermal stress normal to the a and c axes, respectively, and are linked to thermal strain through η. Just as a mechanical stress state involving positive stress along both axes could result in negative strain along c due to coupling through S_{13}, thermal stress driven by positive γ_{blk}^a and γ_{blk}^c could result in $\alpha_c < 0$, where the sign of α_c depends on a careful balance between *all* of S_{ij}, γ_{blk}^a and γ_{blk}^c.

Understanding that NTE in PbTiO₃ arises from a careful balance between S_{ij}, γ_{blk}^a, and γ_{blk}^c terms, we can explore the origin of the sign and magnitude of these parameters through investigating a similar ABO_3 perovskite, SnTiO₃. Previous *ab initio* studies predict that SnTiO₃ also adopts a $P4mm$ ground state structure at 0 K [44]. Though synthesis of bulk SnTiO₃ has proven difficult [45, 46] and few reliable experimental measurements of physical properties exist, it still provides a useful comparison to illuminate the origin of NTE in PbTiO₃. We find that within the QHA, SnTiO₃ exhibits repressed NTE behavior compared to PbTiO₃, and positive or near-zero volumetric NTE at every temperature (see SI).

The behavior of SnTiO₃ can be linked to terms in the compliance matrix (Table I) and bulk Grüneisen tensor ($\gamma_{\text{blk}}^c = 7.72$, $\gamma_{\text{blk}}^a = 3.42$). SnTiO₃ has similar compliance as PbTiO₃ along the a axis, but is much stiffer (lower compliance) along c and exhibits much less coupling between stress along a and strain along c (a lower S_{13}). SnTiO₃ exhibits a slightly more positive γ_{blk}^a at 300 K than PbTiO₃ (3.42 to 1.42), but a γ_{blk}^c over an order of magnitude larger (7.72 to 0.40). Referring to Eqs. (7) and (6), we can confirm that these differences should result in a system where NTE is suppressed compared to PbTiO₃.

As γ_{blk}^a and γ_{blk}^c are vibrational, dynamic properties, the difference between these values in each material could be due to either the mass difference between Sn and Pb (118.71 a.u. and 207.2 a.u., respectively) or from differences in electronic structure, primarily the tendency of the A-site cation to form stereochemically active lone

pairs. We rule out mass difference as the driving effect by performing a computational "experiment" in which the QHA is performed for PbTiO₃, but with the mass of Pb changed to that of Sn (see SI). PbTiO₃ then exhibits lattice parameters as a function of temperature nearly identical to those for the original system in Figure 1, and a 500-700 K α_v of $-2.38 \times 10^{-5} K^{-1}$, which is within 5% of α_v for the original system. Though this experiment is not physically realizable, the results show that the absence of NTE in SnTiO₃ cannot be due to the mass difference between Pb and Sn alone.

Previous studies [47–50] have shown that the ns^2np^0 lone electron pair on Pb and Sn is stereochemically active and is responsible for driving the symmetry-breaking distortion that lowers the symmetry of each material from cubic to tetragonal. The Pb/Sn-s-anion-p interaction at the top of the valence band is actually antibonding and therefore energetically destabilizing. These states could be stabilized by mixing with the unfilled Pb/Sn-p states at the bottom of the conduction band, but such mixing is forbidden by symmetry in the cubic perovskite structure. This electronic instability (known as a pseudo- or second-order Jahn-Teller distortion) manifests in the lattice as a structural phase transition: the ferroelectric transition lowers the atomic site symmetries such that Pb/Sn-s-anion-p-Pb/Sn-p mixing is allowed. The resulting localized, non-bonding state at the top of the valence band is the lone pair.

The closer the cation-s and anion-p states are in energy, the more cation-s character will be present in the anti-bonding states, and the greater the stabilization gained from hybridization between these anti-bonding states and the unfilled cation-p states. Since the Sn $5s$ states are closer in energy to the O $2p$ states than the Pb $6s$ states are [47], SnTiO₃ exhibits a stronger tendency towards a structural distortion than PbTiO₃. In fact, Crystal Orbital Hamiltonian Population (COHP) analysis [51–54] shows that while the Jahn-Teller distortion makes the Pb-s – O-p interaction slightly less antibonding, in the case of SnTiO₃, it brings the Sn-s – O-p interaction from antibonding in the cubic phase to bonding in the tetragonal phase. Since these states are filled, there is a larger energy gain associated with the Jahn-Teller distortion in SnTiO₃ compared with PbTiO₃, and a larger corresponding structural distortion.

Next, we link the size of the structural distortion in SnTiO₃ to S_{13} and its NTE behavior. It is well known in the ferroelectrics literature [55, 56] that c/a in tetragonal BaTiO₃ can be enhanced signficantly with epitaxial strain, thereby signficantly enhancing ferroelectric polarization. In contrast, c/a (and therefore polarization) in PbTiO₃ is quite insensitive to epitaxial strain. This behavior is attributed to the fact that PbTiO₃ in the tetragonal phase is already very structurally distorted, and hence resists further distortions. Since c/a for SnTiO₃ (1.18) is larger than PbTiO₃ (1.08), we predict that S_{13}

for SnTiO$_3$ is less negative than for PbTiO$_3$ because SnTiO$_3$ is *eve more* resistant to further structural distortions than PbTiO$_3$. We tested this hypothesis by calculating selected elements of the compliance tensor for a hypothetical SnTiO$_3$ structure with a c/a ratio set to that of PbTiO$_3$. Compared with SnTiO$_3$ with its equilibrium c/a, this hypothetical structure has a more negative S_{13}, a larger (more positive) S_{33}, and a γ^c_{bulk} of -1.71. Inserting these values of S_{ij} and Grüneisen parameters into Eq. (5) and (6), we find α_a = 7.5 ($\times 10^{-4}$K^{-1}) and α_c = -26.0 ($\times 10^{-4}$K^{-1}). Since $\alpha_v \equiv 2\alpha_a + \alpha_c$, this hypothetical SnTiO$_3$ structure should exhibit volumetric negative thermal expansion. Hence, the electronic structure of the material is important in determining the size of the structural distortion away from the high-symmetry phase. However, in the distorted structure, it is primarily the *shape* of the unit cell that determines the elastic properties and Grüneisen parameters (see SI for further details).

Our results suggest that revisiting anisotropic systems with positive bulk Grüneisen parameters may be a promising direction in the search for new NTE materials. Since the number of unique indices of and $\gamma^{ij}_{\mathrm{b}\,\mathrm{lk}}$ are larger for Bravais lattices of lower symmetry, the number of degrees of freedom in expressions like Eq. (7) increases, providing more pathways for NTE. We have also shown that, critically, as volumetric NTE arises from the product of multiple $\gamma^{ij}_{\mathrm{b}\,\mathrm{lk}}$ and S_{ij}, a search for NTE materials that prioritizes *either* large magnitudes *or* particular signs of certain indices of these tensors will miss favorable candidates. dditionally, in light of previous work [57] suggesting that the presence of lone pair electrons reduces thermal conductivity, exploring the link between phonon modes driving NTE in PbTiO$_3$ and those driving thermal expansion could yield new insights with respect to mode-level control of thermal properties.

* etr38@cornell.edu
† nbenedek@cornell.edu

[1] K. Scheel, Verh. Deutsch. Phys. Ges **9**, 719 (1907).
[2] K. Scheel, Verh. Deutsch. Phys. Ges **9**, 3 (1907).
[3] C. É. Guillaume, CR cad. Sci **125**, 18 (1897).
[4] J. Bruno, N. llan, T. Barron, and . Turner, Phys. Rev. B **58**, 8416 (1998).
[5] . L. Goodwin, M. Calleja, M. J. Conterio, M. T. Dove, J. S. Evans, D. . Keen, L. Peters, and M. G. Tucker, Science **319**, 794 (2008).
[6] D. Dubbeldam, K. S. Walton, D. E. Ellis, and R. Q. Snurr, ngew. Chem. Int. Ed. **119**, 4580 (2007).
[7] S. S. Han and W. . Goddard, J. Phys. Chem. C **111**, 15185 (2007).
[8] H. Jiang, B. Liu, Y. Huang, and K. Hwang, J. Eng. Mater. Technol. **126**, 265 (2004).
[9] S. Biernacki and M. Scheffler, Phys. Rev. Lett. **63**, 290 (1989).
[10] G. Dolling and R. Cowley, Proc. Phys. Soc. **88**, 463 (1966).
[11] G. Barrera, J. Bruno, T. Barron, and N. llan, J. Phys. Condens. Matter **17**, R217 (2005).
[12] C. Lind, Materials **5**, 1125 (2012).
[13] T. Barron, J. Collins, and G. White, dv. Phys. **29**, 609 (1980).
[14] M. G. Tucker, . L. Goodwin, M. T. Dove, D. . Keen, S. . Wells, and J. S. Evans, Phys. Rev. Lett. **95**, 255501 (2005).
[15] M. van Schilfgaarde, I. brikosov, and B. Johansson, Nature **400**, 46 (1999).
[16] . K. Pryde, K. D. Hammonds, M. T. Dove, V. Heine, J. D. Gale, and M. C. Warren, Phase Transitions **61**, 141 (1997).
[17] W. Miller, C. Smith, D. Mackenzie, and K. Evans, J. Mater. Sci. **44**, 5441 (2009).
[18] K. lexandra, K. D. Hammonds, M. T. Dove, . Pryde, V. Heine, J. Gale, and M. Warren, J. Phys. Condens. Matter **8**, 10 (1996).
[19] T. Mary, J. Evans, T. Vogt, and . Sleight, Science **272**, 90 (1996).
[20] K. D. Hammonds, . Bosenick, M. T. Dove, and V. Heine, m. Mineral. **83**, 476 (1998).
[21] P. Lightfoot, D. . Woodcock, M. J. Maple, L. . Villaescusa, and P. . Wright, J. Mater. Chem. **11**, 212 (2001).
[22] . L. Goodwin, K. W. Chapman, and C. J. Kepert, J. m. Chem. Soc. **127**, 17980 (2005).
[23] Y. Yamamura, S. Ikeuchi, and K. Saito, Chem. Mater. **21**, 3008 (2009).
[24] R. Mittal, M. Gupta, and S. Chaplot, Prog. Mater. Sci. **92**, 360 (2017).
[25] R. McCammon and G. White, Philos. Mag. **11**, 1125 (1965).
[26] G. White, J. Phys. C **5**, 2731 (1972).
[27] M. T. Dove and H. Fang, Rep. Prog. Phys. **79**, 066503 (2016).
[28] C. bilitt, S. Craddock, M. S. Senn, . . Mostofi, and N. C. Bristowe, npj Comp. Mat. **3**, 44 (2017).
[29] M. Senn, . Bombardi, C. Murray, C. Vecchini, . Scherillo, X. Luo, and S. Cheong, Physical review letters **114**, 035701 (2015).
[30] P. Giannozzi, S. Baroni, N. Bonini, M. Calandra, R. Car, C. Cavazzoni, D. Ceresoli, G. L. Chiarotti, M. Cococcioni, I. Dabo, *et al.*, J. Phys. Condens. Matter **21**, 395502 (2009).

[31] K. F. Garrity, J. W. Bennett, K. M. Rabe, and D. Vanderbilt, Comput. Mater. Sci. **81**, 446 (2014).

[32] W. Kohn and L. J. Sham, Phys. Rev. **140**, 1133 (1965).

[33] M. Ernzerhof and G. E. Scuseria, J. Chem. Phys. **110**, 5029 (1999).

[34] Z. Wu and R. E. Cohen, Phys. Rev. B **73**, 235116 (2006).

[35] G. Shirane and S. Hoshino, J. Phys. Soc. Jpn. **6**, 265 (1951).

[36] J. Chen, X. Xing, R. Yu, and G. Liu, ppl. Phys. Lett. **87**, 231915 (2005).

[37] T. Barron and R. Munn, Philos. Mag. **15**, 85 (1967).

[38] C. P. Romao, Phys. Rev. B **96**, 134113 (2017).

[39] P. Ghosez, E. Cockayne, U. V. Waghmare, and K. M. Rabe, Phys. Rev. B **60**, 836 (1999).

[40] N. W. shcroft and N. D. Mermin, *Solid State Physics* (Holt, Rinehart and Winston, New York, 1976).

[41] D. C. Wallace, *Thermodynamics of Crystals* (Wiley, 1972).

[42] R. Munn, J. Phys. C: Solid State Physics **5**, 535 (1972).

[43] . Kalinichev, J. Bass, B. Sun, and D. Payne, JMR **12**, 2623 (1997).

[44] W. D. Parker, J. M. Rondinelli, and S. Nakhmanson, Phys. Rev. B **84**, 245126 (2011).

[45] S. F. Matar, I. Baraille, and M. Subramanian, J. Chem. Phys. **355**, 43 (2009).

[46] Y. Konishi, M. Ohsawa, Y. Yonezawa, Y. Tanimura, T. Chikyow, T. Wakisaka, H. Koinuma, . Miyamoto, M. Kubo, and K. Sasata, MRS Proc. **748** (2002).

[47] . Walsh, D. J. Payne, R. G. Egdell, and G. W. Watson, Chem. Soc. Rev. **40**, 4455 (2011).

[48] M. W. Stoltzfus, P. M. Woodward, R. Seshadri, J.-H. Klepeis, and B. Bursten, Inorg. Chem. **46**, 3839 (2007).

[49] K. C. Pitike, W. D. Parker, L. Louis, and S. M. Nakhmanson, Phys. Rev. B **91**, 035112 (2015).

[50] U. Waghmare, N. Spaldin, H. Kandpal, and R. Seshadri, Phys. Rev. B **67**, 125111 (2003).

[51] R. Dronskowski and P. E. Blöchl, J. Phys. Chem. **97**, 8617 (1993).

[52] V. L. Deringer, . L. Tchougréeff, and R. Dronskowski, J. Phys. Chem. **115**, 5461 (2011).

[53] S. Maintz, V. L. Deringer, . L. Tchougréeff, and R. Dronskowski, J. Comput. Chem. **34**, 2557 (2013).

[54] S. Maintz, V. L. Deringer, . L. Tchougréeff, and R. Dronskowski, J. Computational Chem. **37**, 1030 (2016).

[55] C. Ederer and N. . Spaldin, Phys. Rev. Lett. **95**, 257601 (2005).

[56] H. N. Lee, S. M. Nakhmanson, M. F. Chisholm, H. M. Christen, K. M. Rabe, and D. Vanderbilt, Phys. Rev. Lett. **98**, 217602 (2007).

[57] M. D. Nielsen, V. Ozolins, and J. P. Heremans, Energy Environ. Sci. **6**, 570 (2013).